104

Reynolds, Pamela

From: on behalf of STIC-EIC2600
To: Jorgensen, Leland
Subject: RE: ILL_Order

ok we will submit your request.

-----Original Message-----
From: Jorgensen, Leland
Sent: Monday, November 10, 2003 11:38 AM
To: STIC-EIC2600
Subject: ILL_Order

ILL Ordering Information:

Art Unit or Location: 2675 CPK2 6V03

Telephone Number: 305-2650

Application Number or Other Order Identifier: 09/874,128

Please find the following: J. Kido, M. Kimura, K. Nagai, Science, vol. 267, 1332 (1995)

Leland R. Jorgensen
United States Patent & Trademark Office
Patent Examiner
AU 2675
leland.jorgensen@uspto.gov
703.305.2650

Software Version 3.2 (University of Bern, Bern, Switzerland, 1990); G. Beutler, I. Bauersima, W. Gurtner, M. Rothacher, T. Schildknecht, in *Lecture Notes in Earth Sciences*, E. Groten and R. Strauss, Eds. (Springer-Verlag, New York, 1988), pp. 363–380.
18. Goddard Space Flight Center VLBI model GLB 753, C. Ma, J. Ryan, D. S. Caprette, NASA Technical Memorandum 104552.
19. We were able to resolve nearly all of the integer cycle ambiguities in 1992 and a significant number in 1990. Ambiguity resolution was not uniformly successful on baselines longer than 50 km or for which there was less than 6 hours of data.
20. G. Beutler, P. Morgan, R. E. Neilan, *GPS World* (February, 1993), p. 40. The 1993 data were reduced with GIPSY software. S. M. Lichten and J. S. Border, *J. Geophys. Res.* **92**, 12751 (1987); S. M. Lichten, *Manuscripta Geodetica* **15**, 159 (1990). We included data from seven global tracking stations to tie the Hawaii network to the IGS reference frame.
21. This procedure is conservative in that it treats any actual deformation occurring during the annual surveys as measurement error.
22. Only two stations are inconsistent with the constant rate model. One of these, HULU, is located within the upper east rift zone and may have been affected by local deformation. We suspect a problem in the 1992 data at the second site, KULN.
23. W. Thatcher, *U.S. Geol. Surv. Prof. Pap.* **1515**, 189 (1990).
24. Y. Okada, *Bull. Seismol. Soc. Am.* **75**, 1135 (1985).
25. W. A. Duffield, *U.S. Geol. Surv. Prof. Pap.* **856**, 1 (1975).
26. H. T. Stearns and W. O. Clark, *U.S. Geol. Surv. Water-Supply Paper 616*, 194 (1930); H. T. Stearns and G. A. MacDonald, *Hawaii Div. Hydrograph. Bull.* **9**, 363 (1946); J. G. Moore and H. L. Krivoy, *J. Geophys. Res.* **69**, 2033 (1964).
27. P. W. Lipman, W. R. Normark, J. G. Moore, J. B. Wilson, C. E. Gutmacher, *J. Geophys. Res.* **93**, 4279 (1988).
28. J. G. Moore *et al.*, *ibid.* **94**, 17465 (1989); J. G. Moore and G. W. Moore, *Science* **226**, 1312 (1984).
29. W. W. Chadwick *et al.*, *U.S. Geol. Surv. Misc. Field Stud. Map MF-2231* (1993); J. R. Smith, Sheet 5, *Hawaii Seafloor Atlas* (Hawaii Institute of Geophysics and Planetology, Honolulu, HI, 1994).
30. J. R. Smith, *Eos* **73**, 507 (1992); W. W. Chadwick, J. G. Moore, C. G. Fox, D. M. Christie, *ibid.*, p. 507.
31. D. A. Swanson, *Science* **175**, 169 (1972); D. Dzurisin, R. Y. Koyanagi, T. T. English, *J. Volcanol. Geotherm. Res.* **21**, 177 (1984).
32. J. H. Dieterich, *J. Geophys. Res.* **93**, 4258 (1988).
33. M. P. Ryan, *ibid.*, p. 4213.
34. A. Borgia, *ibid.* **99**, 17791 (1994); D. A. Clague and R. P. Denlinger, in preparation.
35. K. Nakamura, *Bull. Volcanol. Soc. Jpn.* **25**, 255 (1980).
36. D. C. Cox, *Source of the Tsunami Associated with the Kalapana (Hawaii) Earthquake of November 1975* (Hawaii Institute of Geophysics, Honolulu, HI, 1980).
37. The August 1990 GPS data were collected under the supervision of J. Dvorak. Thanks to V. Smith, L. Liu, E. Yu, and A. Okamura for help in collecting the field data. P. Okubo provided the earthquake summary data shown in Fig. 1. J. Smith provided the digital topographic and bathymetric data in Fig. 1. Thanks to T. Duennebier for help with graphics and to Y. Bock for providing cleaned GPS tracking data for August 1990. Thanks to P. Delaney and D. Swanson for comments on an early draft of the manuscript.

9 September 1994; accepted 1 December 1994

Multilayer White Light–Emitting Organic Electroluminescent Device

Junji Kido, Masato Kimura, Katsutoshi Nagai

Organic electroluminescent devices are light-emitting diodes in which the active materials consist entirely of organic materials. Here, the fabrication of a white light–emitting organic electroluminescent device made from vacuum-deposited organic thin films is reported. In this device, three emitter layers with different carrier transport properties, each emitting blue, green, or red light, are used to generate white light. Bright white light, over 2000 candelas per square meter, nearly as bright as a fluorescent lamp, was successfully obtained at low drive voltages such as 15 to 16 volts. The applications of such a device include paper-thin light sources, which are particularly useful for places that require lightweight illumination devices, such as in aircraft and space shuttles. Other uses are a backlight for liquid crystal display as well as full color displays, achieved by combining the emitters with micropatterned color filters.

Electroluminescent (EL) devices based on organic thin layers are one of the most promising next-generation flat panel display systems. These devices can be made into large-area, extremely thin full color displays that can be operated by batteries. The structure of the devices is simple, having organic thin layers sandwiched between two electrodes. Because organic layers can be formed by vacuum evaporation or solution casting, the fabrication cost could be less than that of the liquid crystal displays, which are today the most widely used flat panel displays.

In organic EL devices, the generation of light is the consequence of the recombination of holes and electrons injected from the electrodes. Such carrier recombination in the organic emitter layer excites the emitting centers. In a chemical sense, the reaction of radical cations (holes) and radical anions (electrons) provides excited molecules that emit light as one of the decay processes. A variety of materials have been investigated as active materials (*1*–*9*), and a number of device structures (*10*–*22*) have been proposed because it is important to find an appropriate device structure to maximize the carrier recombination efficiency.

The use of multilayer structures was first demonstrated by Tang and VanSlyke (*1*). They used a hole-transport layer for hole injection from the electrode into the electron-transporting emitter layer, which significantly improved the EL efficiency to 1.5 lm/W. Bright electroluminescence of over 1000 cd/m^2, which is high enough for practical applications, with a voltage below 10 V was achieved first. Their device consisted of two active layers with an organic hole-transport layer and an electron-transporting luminescent metal complex layer. The hole-transport layer plays an important role not only in transporting holes but also in blocking electrons, thus preventing electrons from moving into the opposite electrode without recombining with holes. The recombination, therefore, mainly takes place in the emitter layer. Since this first device, various types of EL devices with a multilayer structure have been reported. For instance, a luminescent hole-transporting material can also be an emitter layer when combined with an appropriate electron-transport layer (*4*, *9*, *13*).

In the above examples, various emitting colors have been obtained, including the three primary colors of blue, green, and red. However, there are few white light–emitting devices owing to the lack of the organic fluorescent dyes with white fluorescence. We have therefore focused on developing white light–emitting EL devices and have recently developed one made from a polymer emitter layer doped with three kinds of fluorescence dyes, each emitting blue, green, or red to produce white light (*17*).

In this study, we developed a device structure with three emitter layers, each emitting in the different region of the visible spectrum to generate white light. In general, organic EL devices are composed of two organic layers, each transporting either holes or electrons. In such a device, one of the two layers functions as an emitter layer and the other as a carrier transport layer. Therefore, the emission color is determined by the fluorescence properties of the emitter material, and the light is of the particular color of the emitting material.

One way to add another emission color to such a device is to dope the emitter layer with a fluorescent dye of a different color. For example, it was demonstrated that, in a device with an electron-transporting green-emitting aluminum chelate emitter and a hole-transport layer, when the chelate layer is partly doped with a red-emitting fluorescent dye, the resulting light becomes a mixture of the lights from the two emitter materials, thus producing yellow light (*12*).

Department of Materials Science and Engineering, Yamagata University, Yonezawa, Yamagata 992, Japan.

In this case, the dopant is excited by the energy transfer from the host aluminum chelate or the direct recombination at the dopant site resulting from carrier trapping, or both.

Another way to alter color is to control the carrier recombination zone so that the recombination takes place in two different layers. In this case, the lights from the two layers are combined to produce the mixed color. We have recently reported the spatial control of the recombination zone by the insertion of a hole-blocking layer between an electron-transport layer and a hole-transport layer (*16*). We showed that 1,2,4-triazole derivative is suitable for the hole-blocking layer and that by inserting a thin layer of triazole, carrier recombination can occur both in an electron-transport layer and a hole-transport layer, thus generating light in both layers.

With these two methods, it is expected that in a device with a hole-transport layer, an electron-transport layer, and a doped layer, all three can be emitter layers when an appropriate thickness of a hole-blocking layer is inserted between the hole-transport layer and the electron-transport layer. Thus, using three emitter layers, generating blue, green, and red light, respectively, we expect white light as a mixture of these three primary colors.

Figure 1 shows the materials used in this study. A hole-transporting triphenyldiamine derivative (TPD) has emission peaks at around 410 to 420 nm, the blue region of the visible spectrum. A hole-blocking 1,2,4-triazole derivative (*p*-EtTAZ) has an emission at around 380 nm that transports electrons and effectively blocks holes. An electron-transporting aluminum complex (Alq) has an emission at 520 nm (green), and Nile Red, which has an emission peak at 600 nm (red), is used as a dopant. Indium-tin oxide (ITO) and a magnesium-silver alloy were used as a hole-injecting contact and an electron-injecting contact, respectively.

In the two-layer systems composed of an electron-transport layer and a hole-transport layer, only one of the two layers works as the emitter layer. Figure 2, spectra A and B, illustrate EL spectra of two of such devices, ITO/TPD (500 Å)/Alq (500 Å)/Mg:Ag and ITO/TPD (500 Å)/*p*-EtTAZ (500 Å)/Mg:Ag. From the device with TPD/Alq, green light originating from Alq is observed, indicating that excitons are generated in the Alq layer and the TPD functions only as a hole-transport layer. In contrast, in the device with TPD/*p*-EtTAZ, purplish blue light from the TPD layer is observed, indicating that *p*-EtTAZ has an electron-transporting tendency and blocks holes. Thus, carrier recombination takes place in the TPD layer and consequently excites TPD. Because the excitation energy level of *p*-EtTAZ (emission wavelength, ~390 nm) is higher than that of TPD, the excited energy is not transferred from TPD to *p*-EtTAZ at the interface. These results demonstrate that both Alq and TPD can function as an emitter when combined with an appropriate carrier transport layer.

In devices having three layers, a thin layer of hole-blocking *p*-EtTAZ is inserted between TPD and Alq. A device with 50 Å of *p*-EtTAZ yields emission mostly from TPD (Fig. 2, spectrum C), implying that the recombination zone is mostly in the TPD layer, whereas a device with a thinner (30 Å) *p*-EtTAZ layer (Fig. 2, spectrum D) exhibits emission from both the TPD and

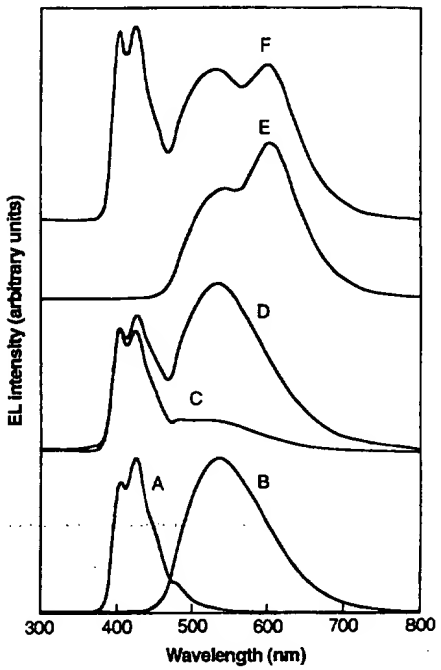

Fig. 2. Electroluminescence spectra for (spectrum A) ITO/TPD (500 Å)/*p*-EtTAZ (500 Å)/Mg:Ag, (spectrum B) ITO/TPD (500 Å)/Alq (500 Å)/Mg:Ag, (spectrum C) ITO/TPD (400 Å)/*p*-EtTAZ (50 Å)/Alq (500 Å)/Mg:Ag, (spectrum D) ITO/TPD (400 Å)/*p*-EtTAZ (30 Å)/Alq (500 Å)/Mg:Ag, (spectrum E) ITO/TPD (400 Å)/Alq (50 Å)/Nile Red–doped (1 mol %) Alq (50 Å)/Alq (400 Å)/Mg:Ag, and (spectrum F) ITO/TPD (400 Å)/*p*-EtTAZ (30 Å)/Alq (50 Å)/Nile Red–doped (1 mol %) Alq (50 Å)/Alq (400 Å)/Mg:Ag cells. These EL spectra were normalized and offset for clarity. All the EL spectra were taken at a current density of 40 mA/cm² with an optical multichannel analyzer (Hamamatsu PMA 10)

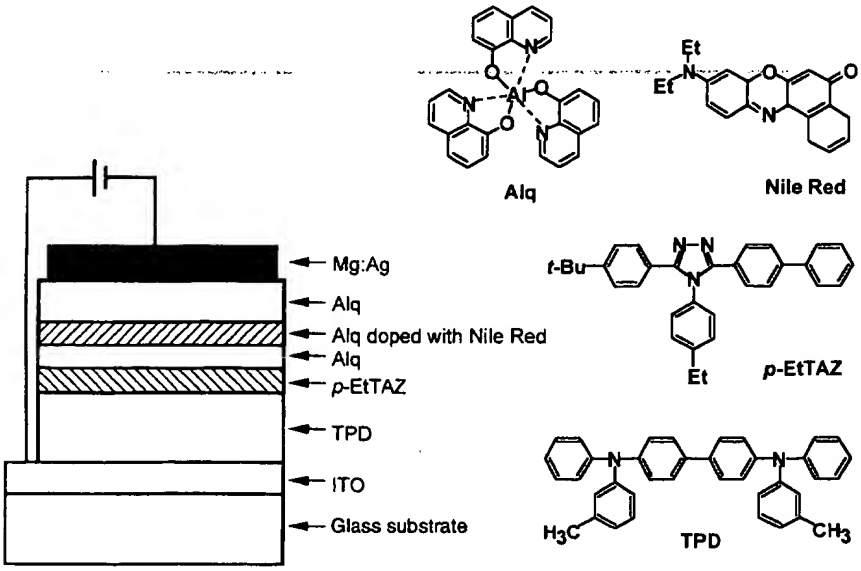

Fig. 1. Configuration of the EL device and molecular structures of materials used. The organic layers were vacuum-deposited on a hole-injecting indium-tin oxide (ITO)–coated glass substrate with a sheet resistance of 15 ohm per square at 10^{-5} torr. The electron-injecting contact was made of an alloy of magnesium and silver (10:1), which was vacuum-deposited from separate sources.

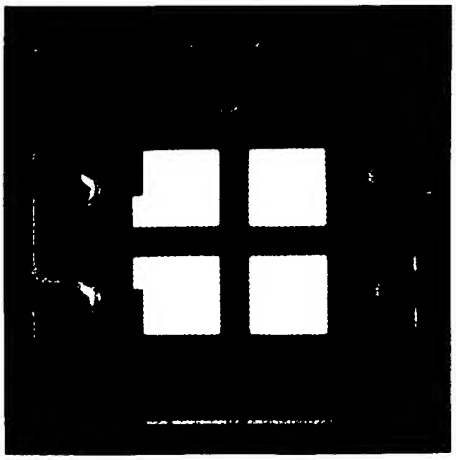

Fig. 3. A photograph of a working white light–emitting EL device. The device is an ITO/TPD (400 Å)/*p*-EtTAZ (30 Å)/Alq (50 Å)/Nile Red–doped (1 mol %) Alq (50 Å)/Alq (400 Å)/Mg:Ag cell. The emitting area is 0.5 cm by 0.5 cm.

the Alq layers. These data indicate that holes can penetrate to some extent when the thickness of the *p*-EtTAZ layer is 30 Å, and the recombination zone locates both in the TPD and Alq layers. Thus, the recombination zone can be spatially controlled by adjusting the thickness of the *p*-EtTAZ layer, and emission from both the hole-transport layer (purplish blue) and the electron-transport layer (green) can be obtained with this device structure. These results are similar to the results obtained with another kind of a triazole derivative (*16*).

Because the device with a *p*-EtTAZ layer 30 Å thick provides bluish green light, the addition of red light should make the output white. To do so, we used the modulation doping technique developed by Tang *et al.* (*12*), in which the Alq layer is doped with Nile Red. Because the emissions from both Alq and Nile Red are necessary, a doped zone 50 Å thick is formed 50 Å away from the interface between the TPD and Alq layers. Thus, the excitons generated in the Alq layer near the interface between TPD and Alq diffuse to the doped layer, exciting the dopants. A TPD/Alq device designed in this manner displays emission from both Alq at 520 nm (green) and Nile Red at 600 nm (red), providing yellow light (Fig. 2, spectrum E). In this case, the dopant molecules are excited by the energy transfer from the host Alq or by direct excitation by carrier recombination at the dopant sites, or both.

Combining the spatial control of the recombination zone and the modulation doping technique, we attempted the generation of white light. The device structure is ITO/TPD (400 Å)/*p*-EtTAZ (30 Å)/Alq (50 Å)/Nile Red–doped (1 mol %) Alq (50 Å)/Alq (400 Å)/Mg:Ag (Fig. 1). Upon the application of dc voltage at ITO positive, white light is observed from the device through the glass substrate (Fig. 3). The EL spectrum (Fig. 2, spectrum F) covers a wide range of the visible region, and three peaks at 410, 520, and 600 nm are seen, corresponding to emission from TPD, Alq, and Nile Red, respectively. In Fig. 4, luminance-voltage and current-voltage characteristics are given. Luminescence starts at a low voltage, such as 6 V, and a maximum luminance of 2200 cd/m^2 is achieved at 16 V. In comparison, the luminance of a cathode ray tube monitor is about 100 cd/m^2. A reasonably high luminous efficiency of 0.5 lm/W is obtained at 12 V. At this drive voltage, the luminance is about 300 cd/m^2. Optimization of the device structure and the use of more suitable materials should provide higher efficiencies, as well as luminance that may exceed 8000 cd/m^2, the luminance of common fluorescent lamps.

We have not measured the lifetime of the device yet; but in general, the stability of organic EL devices have been improving these days. Ten thousand hours of continuous operation has been reported (*22*). Because organic materials have flexibility in material design, an unlimited number of organic materials can be synthesized for the EL application, which is one of their major advantages over inorganic materials. Thus, the possibility of developing organic EL devices having practical durability is quite high.

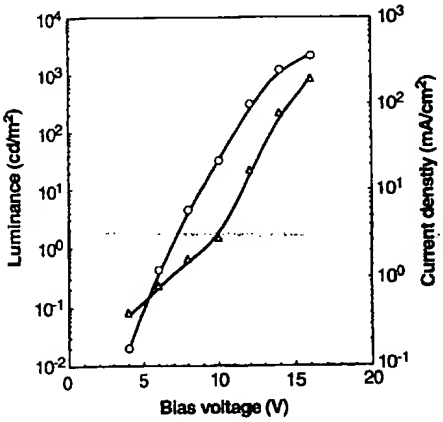

Fig. 4. Luminance-voltage (circles) and current-voltage (triangles) characteristics of a white light–emitting EL device. Luminance was measured at room temperature with a Minolta LS-100 luminance meter.

REFERENCES AND NOTES

1. C. W. Tang and S. A. VanSlyke, *Appl. Phys. Lett.* **51**, 913 (1987).
2. C. Adachi, T. Tsutsui, S. Saito, *ibid.* **56**, 799 (1990).
3. J. H. Burroughes *et al.*, *Nature* **347**, 539 (1990).
4. J. Kido, K. Nagai, Y. Okamoto, T. Skotheim, *Chem. Lett.* **1991**, 1267 (1991).
5. ———, *Appl. Phys. Lett.* **59**, 2760 (1991).
6. Y. Hamada, C. Adachi, T. Tsutsui, S. Saito, *Jpn. J. Appl. Phys.* **31**, 1812 (1992).
7. N. C. Greenham *et al.*, *Nature* **365**, 628 (1993).
8. E. Aminaka, T. Tsutsui, S. Saito, *Jpn. J. Appl. Phys.* **33**, 1061 (1994).
9. J. Kido, K. Hongawa, K. Okuyama, K. Nagai, *Appl. Phys. Lett.* **63**, 2627 (1993).
10. C. Adachi, S. Tokito, T. Tsutsui, S. Saito, *Jpn. J. Appl. Phys.* **27**, L268 (1988).
11. ———, *ibid.*, p. L713.
12. C. W. Tang, S. A. VanSlyke, C. H. Chen, *J. Appl. Phys.* **65**, 3610 (1989).
13. C. Adachi, T. Tsutsui, S. Saito, *Appl. Phys. Lett.* **55**, 1489 (1989).
14. J. Kido, M. Kohda, K. Okuyama, K. Nagai, *ibid.* **61**, 761 (1992).
15. J. Kido, M. Kohda, K. Hongawa, K. Okuyama, K. Nagai, *Mol. Cryst. Liq. Cryst.* **227**, 277 (1993).
16. J. Kido, C. Ohtaki, K. Hongawa, K. Okuyama, K. Nagai, *Jpn. J. Appl. Phys.* **32**, L917 (1993).
17. J. Kido, K. Hongawa, K. Okuyama, K. Nagai, *Appl. Phys. Lett.* **64**, 815 (1994).
18. M. Era, S. Morimoto, T. Tsutsui, S. Saito, *ibid.* **65**, 676 (1994).
19. V. L. Colvin, M. C. Schlamp, A. P. Alivisatos, *Nature* **370**, 354 (1994).
20. C. Morishima, M. Yoshida, A. Fujii, Y. Ohmori, K. Yoshino, *Jpn. J. Appl. Phys.* **33**, L1228 (1994).
21. J. Kido, H. Hayase, K. Hongawa, K. Nagai, K. Okuyama, *Appl. Phys. Lett.* **65**, 2124 (1994).
22. Y. Shirota *et al.*, *ibid.*, p. 807.

21 October 1994; accepted 23 December 1994

A Structure Model and Growth Mechanism for Multishell Carbon Nanotubes

S. Amelinckx,* D. Bernaerts, X. B. Zhang, G. Van Tendeloo, J. Van Landuyt

A model that postulates a mixture of scroll-shaped and concentric, cylindrical graphene sheets is proposed to explain the microstructure of graphite multishell nanotubes grown by arc discharge. The model is consistent with the observed occurrence of a relatively small number of different chiral angles within the same tubule. The model explains clustering in a natural way and is consistent with the observation of asymmetric (0002) lattice fringe patterns and with the occurrence of singular fringe spacings larger than *c*/2 (*c* is the *c* parameter of graphite) in such patterns. Anisotropic thermal contraction accounts for the 2 to 3 percent increase in the *c* parameter of nanotubes, compared with bulk graphite, but is too small to explain the singular fringe spacings. The model also explains the formation of multishell closure domes. Nucleation is attributed to the initial formation of a fullerene "dome."

Iijima (*1*) found that nanometer-thin, micrometer-long tubes consisting of concentric, cylindrical graphene sheets are formed as a by-product of the arc-discharge synthesis of fullerenes (*2*). These tubes have a chiral character (*1*) that can determine their electronic properties (*3*). Electron diffraction studies showed that many multisheet tubules contain achiral as well as chiral tubes (*4*, *5*). A multilayer tubule may exhibit several chiral angles, their number being very often 1/2 to 1/5 the number of sheets, suggesting that the sheets occur in clusters with the same chirality. It was proposed (*4*, *5*) that the chirality is a means of accommodating

Electron Microscopy for Materials Research, University of Antwerp (RUCA), Groenenborgerlaan 171, B-2020 Antwerp, Belgium.

*To whom correspondence should be addressed.